From Lamb waves to quasi-guided waves: On the wave field and radiation of elastic and viscoelastic plates

Daniel A. Kiefer*, Michael Ponschab, Stefan J. Rupitsch

Friedrich-Alexander-University Erlangen-Nürnberg (FAU), Sensor Technology, 91052 Erlangen, Germany

Abstract

Leaky Lamb waves are elastodynamic quasi-guided waves propagating in plates which are in contact with a fluid. They are usually perceived and studied as perturbations to waves in the free plate. Recent advances in solving the nonlinear eigenvalue problem that describes these waves allow to reliably and efficiently obtain all solutions. The resulting wavenumbers in the plate and in the fluid as well as the wave field account for the exact fluid-structure interaction. A classification of the solutions based on the transversal wavenumber spectrum is proposed. The properties of each kind of quasi-guided wave are discussed. Moreover, we analyze the relationship between radiation rate and attenuation. The free, perfectly elastic plate exhibits wave propagation without losses. Nontheless, attenuated modes exist in this case and are known as nonpropagating modes. We show that – in contrast to the free plate – attenuation of waves is solely due to radiation, that all waves propagate energy and that subsonic radiation is possible. The radiation rate of the waves can be calculated using their eigenvector. This allows to split the total attenuation of waves in viscoelastic plates into a contribution due to radiation and one due to damping. Lastly, we present and discuss the dispersion curves of a strongly fluid-loaded plate.

Keywords: guided wave, leaky Lamb wave, fluid-coupled plate, radiation, open domain problem

1. Introduction

Thin structures act – intentionally or unintentionally – as mechanical waveguides. Modeling and analysis of these waveguides has become important in nondestructive testing and ultrasonic sensor design. The interaction of the structure with an adjacent fluid is thereby often of utmost importance for sensor and nondestructive testing applications [1].

The fluid-coupled plate is the simplest of all open mechanical waveguides and it is a very adequate prototype to study the physical properties of leaky guided waves. We call the waveguide "open" because energy may be exchanged with the surrounding infinite fluid domain. Consequently, most waves in this system do not conserve the energy within the mechanical structure as they propagate and we call them *quasi-guided waves*. The waves that supply energy to the fluid domain are referred to as *leaky waves*.

Classically, fluid-loading of plates was studied by perturbation of the free plate solutions [2–6]. This only represents a good approximation for "slightly fluid-loaded" plates, i.e., when the mechanical parameters of the plate and the fluid exhibit a strong mismatch. Exact solutions of the frequency-dependent wavenumbers of leaky Lamb waves have been studied by zero-finding of the transcendental characteristic equations [4, 7–11]. More recently, solution methods based on discretizing the nonlinear eigenvalue problem have been presented [12–14]. Alternatively, fluid-coupled plates can also be studied using Perfectly Matched Layers [15, 16], which yields some solutions of the finite but open domain problem (trapped and leaky waves) mixed with those of the infinite domain problem (trapped waves and radiation modes) [15]. Only few studies exist that explicitly examine the wave field and energy flux of leaky Lamb waves, concentrating mainly on backward waves [17–19].

Recently we presented a numerical solution methods that enables us to reliably find all solutions as a full set of eigenvalues (wavenumbers) and eigenvectors (wave field) [12]. Coupling a mechanical waveguide to a surrounding fluid fundamentally changes the plane harmonic waves solutions, both from a physical and a mathematical point of view. This contribution relates the exact and complete solutions of the fluid-coupled plate to the well-known free plate solutions. The analysis is performed mainly from a physical point of view. In particular, a detailed analysis relates the acoustic radiation to the complex wavenumber spectrum – an important step that is missing in the literature, presumably because it "seems natural" to obtain a complex wavenumber spectrum. Moreover, we propose a classification of the quasi-guided waves based on the transversal wavenumbers.

Before introducing the concept of quasi-guided waves in Section 3, we provide a short review of Lamb waves in a free plate in Section 2, which serves as reference for the upcoming discussions. Section 4 examines general properties of quasi-guided waves, introduces a classification and explicitly discusses each kind of solution. Section 5 relates the radiation properties of leaky waves to the wavenumbers on a physical basis. Thereby,

*Corresponding author
Email address: daniel.kiefer@fau.de (Daniel A. Kiefer)

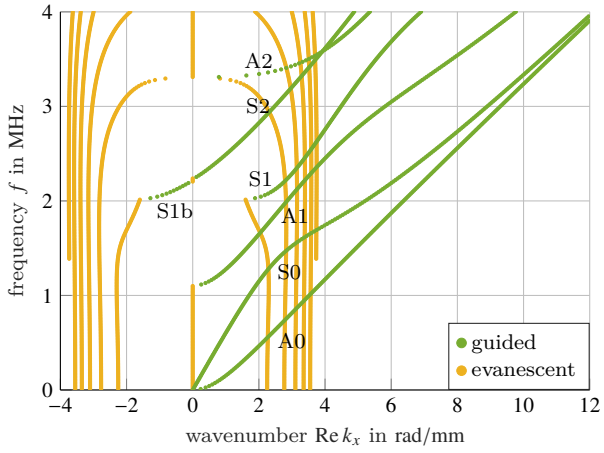

(a)

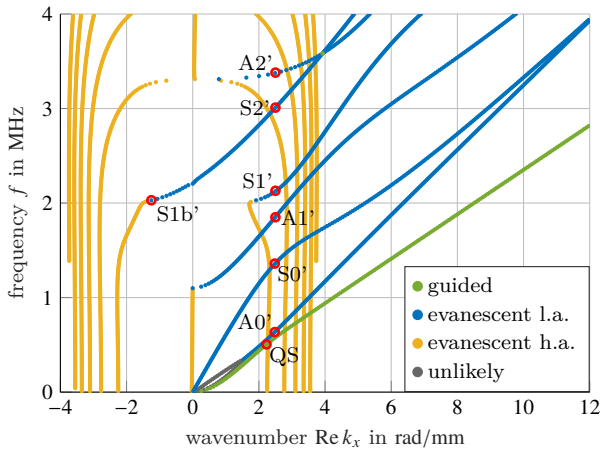

(b)

Figure 1: Comparison of the wavenumbers of a 1 mm thick brass plate: (a) traction free plate, (b) plate in contact with water on one side. The evanescent waves have been classified into "lowly attenuated" (l.a.) and "highly attenuated" (h.a.) with a threshold of 0.2 Np/mm for comparison only.

fundamental differences to the free plate solutions are revealed and discrepancies to standard (approximative) analysis procedures are discussed. Lastly, we extend the leaky wave discussion to dissipative plates and to strongly-fluid loaded plates in Section 6 and Section 7, respectively.

2. Review of the free plate spectrum

Throughout this contribution, the solutions of the fluid-coupled plate will be compared to the ones of the free plate, i.e., without traction at the surfaces. For the sake of reference, the well-known Lamb wave solutions of the free plate will be presented shortly [2, 20, 21]. Their frequency-dependent complex wavenumbers $k_x(f)$ – called the *spectrum* – constitute a set of curves in the three-dimensional space $[f \times \mathrm{Re}\, k_x \times \mathrm{Im}\, k_x]$ [21], where "Re" and "Im" refer to the real and imaginary parts, respectively. Each curve corresponds to one *normal mode* [2, 22, 23], i.e., the solutions form an orthogonal basis able to represent any arbitrary field inside the plate. The projection of the dispersion curves of a 1 mm thick brass plate (Young's modulus $E = 110\,\mathrm{GPa}$, Poisson's ratio $\nu = 0.34$, mass density $\rho = 8440\,\mathrm{kg/m^3}$) onto the $[f \times \mathrm{Re}\, k_x]$-plane is shown in Fig. 1a. Throughout this paper, we will restrict the discussion to solutions that propagate energy in positive x-direction. Only these solutions are shown in Fig. 1 and all other graphs, although corresponding waves carrying energy in the opposite direction exist due to the geometric symmetry of the problem.

The spectrum of the free plate splits into a finite number of *propagating* or *guided* modes (Fig. 1a, ●) and an infinite number of *nonpropagating* or *evanescent* modes [24] (Fig. 1a, ●). While the former propagate energy, the latter are characterized by zero energy velocity/group velocity [2, 24]. Additionally, the nonpropagating modes always exhibit attenuation, i.e., $\mathrm{Im}\, k_x > 0$, while the propagating modes have real-valued wavenumbers [24]. The propagating modes are actual waves, while the nonpropagating modes represent local vibrations of the plate [25, 26], i.e., vibrations in the near-field of a source.

Waves with positive $\mathrm{Re}\, k_x$ have a positive phase velocity $c_\mathrm{p} = \omega/\mathrm{Re}\, k_x$ and are called *forward waves*. But waves with negative wavenumber $\mathrm{Re}\, k_x$ also exist and they are called *backward waves* [24] because their phases propagate in the opposite direction as compared to the propagation of energy. Solutions with zero wavenumbers are also found. These represent uniform vibrations of the entire plate and their wavelength tends to infinity [27].

3. Quasi-guided waves in fluid-coupled plates

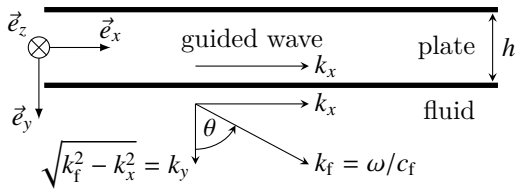

Figure 2: Cross-sectional detail of the plate with thickness h and infinite extend in the x-z-plane. The plate is in contact with a fluid at the bottom.

Let us consider the geometry depicted in Fig. 2. The plate of thickness h and otherwise unbounded extend consists of a homogeneous and isotropic solid material. The solid layer is in contact with an infinite fluid domain on the bottom surface. It is straight forward to extend the problem to fluid coupling on both sides. The wave motions are purely in the x-y-plane, i.e., a plane strain state [28, 29] is assumed. Due to the translational symmetry in time t and the spacial coordinate x, it is possible to seek mechanical displacements $\vec{u}$ of the form [30]

$$\vec{u} = \vec{u}(y)\, \mathrm{e}^{\mathrm{i}(k_x x - \omega t)}\,,\ k_x \in \mathbb{C}\,,\ \omega, x, t \in \mathbb{R}\,. \tag{1}$$

This reduces the corresponding equations of free motion to an eigenvalue problem on the one-dimensional domain $y \in [-h/2, \infty)$ parameterized in the angular frequency $\omega = 2\pi f$ and the complex wavenumber k_x. We consider k_x to be the eigenvalue and $\vec{u}(y)$ the eigenfunction, while ω is a free parameter. The possible combinations of ω and k_x values are called the

dispersion curves and they are described by the *dispersion relation* [2, 31].

Two non-equivalent and conceptually different approaches exist to find a dispersion relation and the corresponding eigenfunctions [15, 30, 32]. The first one considers the infinite fluid domain in addition to the plate as described above. This yields the "modes of the universe" [32, 33], which involves a continuous set of *radiation modes* as well as a discrete set of *trapped modes* [15, 32]. This uncountable infinite modal basis is capable of fully describing the wave field and its dynamics in both the plate and the fluid domain. However, the resonances of the plate – which are of interest in nondestructive testing and sensor applications – remain hidden in the continuum of the radiation modes [32, 34].

The second model restricts attention to the plate itself by considering only its interaction with the fluid. It gets rid of the surrounding fluid domain by imposing appropriate boundary conditions [32, 33] on the plate's domain. This results in a non-conservative system with a discrete set of eigensolutions, namely the *quasi-guided waves*. The solutions do not represent modes in the usual sense [30] – although they might when introducing appropriate concepts [32] – a matter that is outside the scope of this paper. They are – at least – resonances that strongly dominate the overall wave field [30, 34] and are easier to deal with as compared to the continuous spectrum of the infinite domain. The concept of quasi-guided waves is the more appropriate one for nondestructive testing and sensor applications because the transmitter and receiver are usually both situated on the plate, which in this formalism is described without the cluttering of modes related to the exterior [16, 32, 34].

In a previous publication by the authors [12], the modeling and solution procedure to compute the quasi-guided waves has been explained in detail. The idea is sketched briefly in the following. It consists in reducing the infinite domain $y \in [-h/2, \infty)$ to the finite domain $y \in [-h/2, h/2] \cup \partial\Omega_\mathrm{f}$, where $\partial\Omega_\mathrm{f}$ represents the fluid boundary interfacing the plate. This is achieved by assuming a-priori an inhomogeneous plane bulk wave [35] in the fluid half-space, i.e., $\vec{u}(y) \sim A\,\mathrm{e}^{\mathrm{i}k_y y}$ on $y \in (h/2, \infty)$, where $k_y \in \mathbb{C}$ is the transversal wavenumber and the amplitude A is the new scalar degree of freedom. The complex wave vector in the fluid domain is, hence, given by $\vec{k}_\mathrm{f} = [k_x, k_y]^T$. Imposing appropriate interface conditions between the plate's domain $[-h/2, h/2]$ and the fluid domain $\partial\Omega_\mathrm{f}$, results in a frequency-dependent *nonlinear, differential eigenvalue problem* [12, 13] for the wavenumbers k_x and the eigenfunctions $[u_x(y), u_y(y), A]^T$ of the quasi-guided waves. After discretization, an algebraic nonlinear eigenvalue problem of the form [12]

$$\left(k_x^2 \underline{\underline{A}}_2 + k_x \underline{\underline{A}}_1 + \underline{\underline{A}}_0 + \mathrm{i}\sqrt{k_\mathrm{f}^2 - k_x^2}\,\underline{\underline{B}}\right)\underline{q} = \underline{0} \tag{2}$$

has to be solved, where $\underline{\underline{A}}_2, \underline{\underline{A}}_1, \underline{\underline{A}}_0$ and $\underline{\underline{B}}$ are constant matrices and $k_\mathrm{f} = |\vec{k}_\mathrm{f}| = \omega/c_\mathrm{f} \in \mathbb{R}$. The solution technique is based on a trigonometric change of variable, namely $k_x = k_\mathrm{f}\frac{\gamma+\gamma^{-1}}{2}$, which enables us to linearize the eigenvalue problem in the variable γ. Remarkably, the employed procedure does not only map γ uniquely to k_x, but also to the transversal wavenumber via $k_y = k_\mathrm{f}\frac{\gamma-\gamma^{-1}}{2\mathrm{i}}$ [12].

4. General properties and classification of quasi-guided waves

The eigensolutions of the same brass plate as in Section 2 but coupled on one side to water (inviscid, longitudinal wave speed $c_\mathrm{l} = 1480\,\mathrm{m/s}$, mass density $\rho = 1000\,\mathrm{kg/m^3}$) has been computed with the described numerical method. The real part of the resulting wavenumbers is displayed in Fig. 1b for comparison with the free plate. In contrast to what is often assumed, the high similarity of the wavenumbers of guided and quasi-guided waves is not a general feature, but rather a property of the "slightly fluid-loaded" plate. We chose this example because it facilitates a comparative discussion of guided and quasi-guided waves. Moreover, we have split evanescent waves into "lowly attenuated" (l.a., ●) and "highly attenuated" (h.a., ●) for the sake of discussion only. The threshold in attenuation is arbitrary and it has been chosen as $0.2\,\mathrm{Np/mm}$ for the given example. Otherwise, the same coloring scheme is used in all figures comparing guided and quasi-guided waves. With this in mind, the transition in the nature of waves due to fluid-loading is clearly visible in Fig. 1 and will be discussed in detail after pointing out the general properties of the obtained solutions. The imaginary part $\mathrm{Im}\,k_x$ of the wavenumbers has a conceptually different physical interpretation as in the free plate case and will be discussed in Subsection 5.2, where they are plotted in Fig. 10.

The eigenfunctions $[u_x(y), u_y(y), A]^T$ that describe the wave field are also obtained by solving the eigenvalue problem. In contrast to the free plate, the complex displacement distributions $u_x(y)$ and $u_y(y)$ in the plate are no longer exactly out of phase [19], accounting for loss of energy to the fluid domain. The geometrically asymmetric setup along $\vec{e}_y$ leads to asymmetric solutions. In case of slight fluid loading, $u_x(y)$ and $u_y(y)$ will still be "predominantly" odd or even in the sense of a decomposition. Therefore, we choose to label the eigensolutions of the water-coupled brass plate with the conventional scheme used for symmetric and anti-symmetric Lamb waves but marked with a ' (see Fig. 1b).

Two representative eigenfunctions are shown in Fig. 3. Note that the field in the fluid domain is determined indirectly by the harmonic extrusion $\vec{u}_\mathrm{f}(y) = \mathrm{i}[k_x, k_y]^T A\,\mathrm{e}^{\mathrm{i}k_y(y-h/2)}$ according to the plane wave assumption. This fact is essential because it allows us to compute and represent the exponentially increasing field of the leaky wave seen in Fig. 3a. Diverging wave fields in the transversal direction are a well-known property of leaky waves [14, 15, 30, 34, 36–39] and is a direct consequence of lossless wave propagation in the fluid, as will be discussed in Section 4.2.

In principle, the y-dependent eigenfunctions are sufficient to describe the plane harmonic wave field. For the purpose of visualization, the wave field can be extruded to the whole x-y-plane using (1). This has been done for the modes marked in Fig. 1b and the resulting displacement fields are shown in Fig. 4.

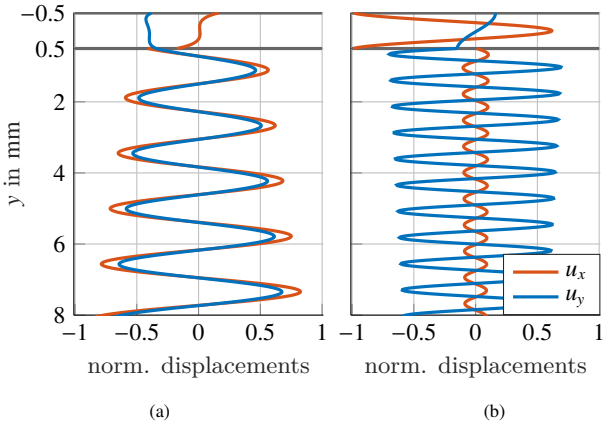

(a) (b)

Figure 3: Transversal displacement distributions of waves radiating into an inviscid fluid: (a) forward wave A0' at 1.5 MHz, (b) backward wave S1b' at 2 MHz.

Due to the non-unique relationship between k_x and k_y, a full description of the dispersion spectrum additionally requires the transversal wavenumbers k_y – these are plotted in the complex plane in Fig. 5. Note that the real and imaginary parts of k_x and k_y are related to each other because plane inhomogeneous waves in an inviscid fluid are known to be restricted to transversal attenuation [35], i.e., along their wave fronts as shown in Fig. 6. This is a consequence of their dispersion relation, given by $\vec{k}_\mathrm{f} \cdot \vec{k}_\mathrm{f} = \omega^2/c_\mathrm{f}^2 \in \mathbb{R}$ [31]. This immediately implies that $\mathrm{Re}\,\vec{k}_\mathrm{f} \cdot \mathrm{Im}\,\vec{k}_\mathrm{f} = 0$. Hence, the attenuation vector $\mathrm{Im}\,\vec{k}_\mathrm{f}$ is always orthogonal to the propagation vector $\mathrm{Re}\,\vec{k}_\mathrm{f}$.

The transversal wavenumbers are not only required to describe the wave field, but are also convenient to classify the solutions. Depending on the far-field behavior, the quasi-guided waves of the fluid-coupled plate can be classified into three kind of waves:

1. Guided/trapped waves: $\mathrm{Re}\,k_y = 0$ and $\mathrm{Im}\,k_y > 0$
2. Leaky/evanescent waves: $\mathrm{Re}\,k_y > 0$
3. Incoming waves: $\mathrm{Re}\,k_y < 0$

The corresponding regions of the complex k_y plane are indicated in Fig. 5, where the leaky waves have been divided again into forward and backward waves (discussed later on). Note that it would also be possible to perform the classification using the wavenumbers k_x, but only after distinguishing between waves that propagate energy in positive and in negative x-direction. Each kind of wave will be discussed separately in the following.

4.1. Guided waves

Properly guided waves of fluid-coupled waveguides are also called *trapped* waves [15]. They have purely real wavenumbers k_x and propagate along the plate without attenuation. These are the only solutions that carry energy towards $x \to \infty$ without external supply of energy [18]. As they do not exchange energy with the fluid medium, their transversal wavenumber k_y must be purely imaginary. We suggest that only

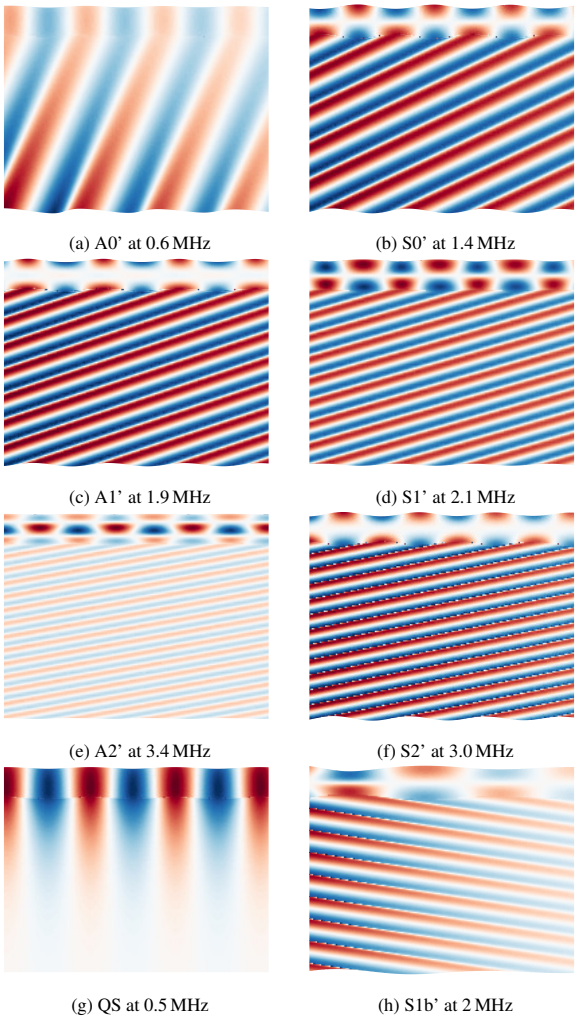

(a) A0' at 0.6 MHz (b) S0' at 1.4 MHz

(c) A1' at 1.9 MHz (d) S1' at 2.1 MHz

(e) A2' at 3.4 MHz (f) S2' at 3.0 MHz

(g) QS at 0.5 MHz (h) S1b' at 2 MHz

Figure 4: Wave fields of the eigensolutions marked in Fig. 1b. The color indicates the u_y displacement.

solutions with $\mathrm{Im}\,k_y > 0$ should be considered physically meaningful and are termed "guided" (●) in this paper and in Fig. 1b. In this case, the wave field decays with distance to the plate and is confined to its proximity [40], as can be observed in Fig. 4g.

For a plate with single-sided slight fluid loading, one guided wave is known and is referred to as *Quasi-Scholte wave* (QS mode) or *A-wave* in the literature [40–42] (● in Fig. 1b and Fig. 5a, as well as Fig. 4g). Note that for double-sided fluid loading, a second Quasi-Scholte wave exists, which is sometimes termed the *S-wave* [9, 41, 43]. More guided waves may exist in plates with stronger fluid loading, as will be shown in Section 7.

Guided wave solutions with $\mathrm{Im}\,k_y < 0$ also exist and are referred to as "unlikely" (●) in Fig. 1b. These physically unlikely solutions appear in the literature [4, 9, 44–46] but their nature is not understood and their existence could not been confirmed experimentally [46]. The fact that they show a diverging wave field in transversal direction is not sufficient to discard the solutions for two reasons: (1) Leaky waves also have this property and (2) the open domain solutions are not able to exactly represent the wave field in the fluid domain anyway. In the dispersion

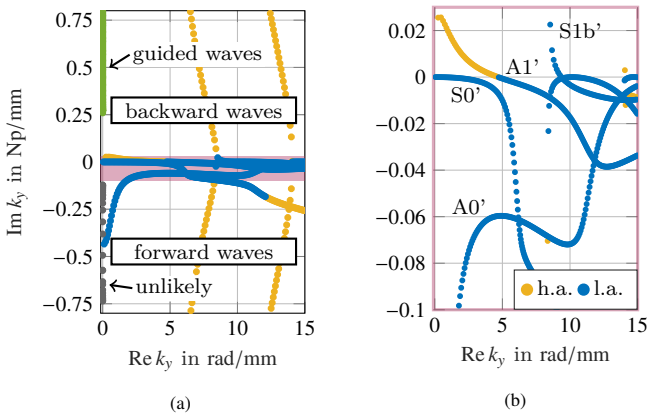

(a) (b)

Figure 5: Transversal wavenumbers $k_y(f)$ in the complex plane indicating the classification of waves: (a) right half of the symmetric k_y-plane, (b) zoom into the shaded region in (a). The quadrants marked "backward waves" and "forward waves" correspond both to leaky waves.

diagrams they tend to form loops, sometimes in conjunction with proper guided wave solutions. For this reason they have been discussed as *real-valued loops* in the literature [44]. It should be mentioned that the physically unlikely solutions and the guided modes are indistinguishable by solely inspecting the k_x-spectrum. This reveals the importance of the k_y-spectrum when classifying the solutions and this is presumably the reason why no discrimination has been made in the literature previously.

4.2. Leaky waves

Leaky or evanescent waves are attenuated along the plate, i.e., $\mathrm{Im}\, k_x > 0$. Often only the "lowly attenuated" evanescent waves are referred to as *leaky Lamb waves* in the literature [8]. Nevertheless, in this contribution we use the term *leaky Lamb waves* to refer to all evanescent waves in the fluid-coupled plate because – as will be shown – they all leak energy into the fluid and these waves are otherwise physically indistinguishable.

Leaky waves can also be characterized through their transversal wavenumber k_y, as their real part must be positive – carrying energy away from the plate. While backward leaky waves are located in the open first quadrant of Fig. 5a, forward leaky waves can be found in the open fourth quadrant. This means that the wave field decreases exponentially with distance to the plate for backward waves, but increases for forward waves as has already been mentioned – observe this behavior by inspecting the displacement structures in Fig. 3a.

To understand the exponential growth in transversal direction, consider the leaky forward wave being attenuated in positive x-direction as sketched in Fig. 6a. The radiated acoustic wave propagates in the inviscid fluid without attenuation in direction $\mathrm{Re}\,\vec{k}_\mathrm{f}$, which forms positive angles with respect to $\vec{e}_y$. Hence, if the wave field gets attenuated along $\vec{e}_x$, than its amplitude must increase along $\vec{e}_y$. The opposite is true for backward waves, whose $\mathrm{Re}\,\vec{k}_\mathrm{f}$ form negative angles with $\vec{e}_y$. This situation is sketched in Fig. 6b. Backward waves that propagate energy in $\vec{e}_x$ are also attenuated in this direction. At the same time

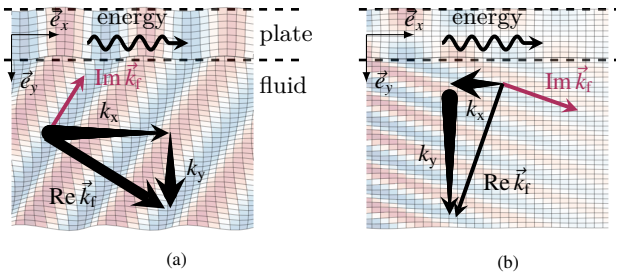

(a) (b)

Figure 6: Wave vector components in the fluid half space for (a) forward wave A0' at 1 MHz and (b) backward wave S1b' at 2.1 MHz. The black arrow's length indicate the propagation constants, i.e., the real parts, while the change in the arrow's thickness illustrate the change in acoustic amplitude, i.e., the imaginary parts. Additionally, the total attenuation vector $\mathrm{Im}\,\vec{k}_\mathrm{f}$ is also drawn.

they exhibit negative $\mathrm{Re}\, k_x$ and, hence, the acoustic field must decrease with distance to the plate.

4.3. Incoming waves

In the context of scattering problems, incoming waves are usually discarded a-priori by imposing a *radiation condition* on the open domain problem [32]. Our solution method simply couples the plate to an inhomogeneous plane wave in the fluid, which might be incoming (carries energy towards the plate) or outgoing (carries energy away, i.e., leaky waves), hence both types of solutions are obtained. Incoming waves describe the excitation of a quasi-guided wave inside the plate due to an incident ultrasonic wave [6]. They are the reciprocal solutions to the leaky waves, featuring complex conjugate wavenumbers k_x. For clarity, they have been omitted in all figures. Due to the supply of energy from the fluid domain, the quasi-guided wave's amplitude inside the plate increases along the direction of energy propagation. Incoming waves have negative $\mathrm{Re}\, k_y$ and they would be located in the omitted open left half-plane of Fig. 5a.

5. Radiation of leaky Lamb waves

Radiation is a mode-conversion process, by which elastodynamic waves inside the plate generate an acoustic wave in the adjacent fluid domain. In this section, we will analyze the radiation of leaky Lamb waves, which is of relevance to many applications considering these kind of waves. To characterize the radiated waves, we will use the radiation angle and the radiation rate.

5.1. Radiation angle

The used solution method provides both wavenumber components k_x and k_y. As the phase fronts of the plane wave in the fluid are described by $\mathrm{Re}\,\vec{k}_\mathrm{f}$, the radiation angle θ with respect to the plate's normal $\vec{e}_y$ can be obtained with (see Fig. 2)

$$\theta = \arctan\left(\frac{\mathrm{Re}\, k_x}{\mathrm{Re}\, k_y}\right). \tag{3}$$

The resulting radiation angles are displayed in Fig. 7. Note that negative radiation angles correspond to backward waves.

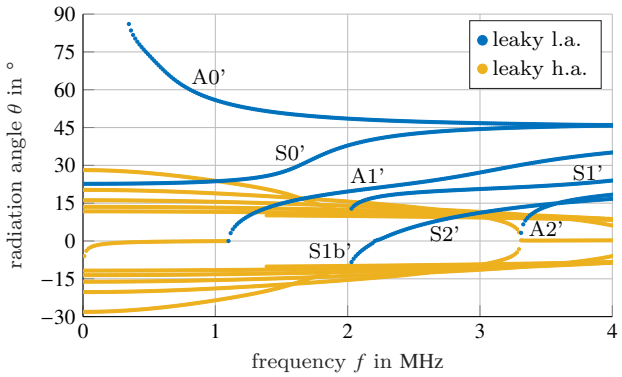

Figure 7: Radiation angles with respect to the plate's normal of a 1 mm thick brass plate in contact on one side with water.

Definition (3) ensures real-valued radiation angles and is equivalent to $\theta = \mathrm{Re}\{\arcsin(k_x/k_\mathrm{f})\}$, given the fact that $\mathrm{Re}\,\vec{k}_\mathrm{f} \perp \mathrm{Im}\,\vec{k}_\mathrm{f}$. However, note that using only the real part of the wavenumber, i.e, $\theta_\mathrm{pert} = \mathrm{Re}\{\arcsin(\mathrm{Re}\,k_x/k_\mathrm{f})\} = \mathrm{Re}\{\arcsin(c_\mathrm{f}/c_\mathrm{p})\}$ – which is often done [5, 6, 20, 23] – is strictly speaking not valid. Naturally, this still yields good approximation for the lowly attenuated modes.

5.2. Radiation rate

The relation between attenuation and rate of energy leakage is discussed in the following. Even a free and lossless plate exhibits attenuated modes, as has been discussed in Section 2. Therefore, the question arises, whether such local vibrations – whose attenuation is not related to radiation nor damping – do exist in the fluid-coupled plate as well [10].

We can describe the leakage of energy using the eigenfunctions $\vec{u}(y)$ and balance of power flux across a section of the waveguide as depicted in Fig. 8. Per propagation length $\mathrm{d}x$, a fraction of the total local elastodynamic power flux $P_x(x)$ inside the plate is radiated as acoustic power $\mathrm{d}P_\mathrm{r}$. This leads to an exponential decay of the wave field due to radiation, i.e., $\vec{u} \sim \mathrm{e}^{-\alpha x}$ and $P_x(x) \sim \mathrm{e}^{-2\alpha x}$. We call α the *radiation rate* and it characterizes how fast energy leaks from the plate into the adjacent fluid. Because we compute α using the power flux through the plate's boundary, it does indeed *only* represent attenuation due to leakage. The total attenuation is given by $\mathrm{Im}\,k_x = \alpha + \beta$, where β is attenuation due to other reasons. In the following, we show numerically that $\beta = 0$ for all solutions of the nondissipative plate.

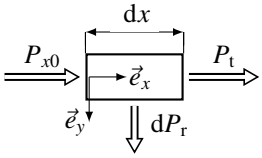

Figure 8: Balance of power flux inside a plate section.

In general, the average power flux density is given by the real part of the elastodynamic Poynting vector $\mathrm{Re}\,\vec{I}$ [31, 47]. These

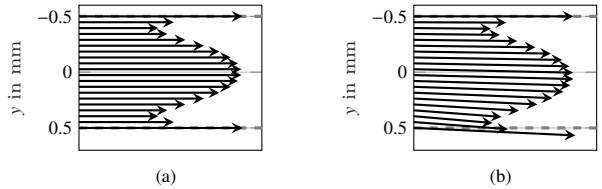

Figure 9: Poynting vectors $\vec{I}_0(y)$ indicating the average local flux of power in magnitude and direction for (a) free plate S0 at 2 MHz mm and (b) water-coupled plate S0' at 2 MHz mm. The plate is located in between $y = -0.5$ mm and $y = -0.5$ mm.

vectors are displayed exemplarily in Fig. 9 and they characterize the local magnitude and direction of power flux. As expected, the power is confined within the free plate (Fig. 9a), but it may flow across the plate-fluid interface (Fig. 9b). Using the stiffness tensor $\mathbf{c}$ of the plate's material, the Poynting vectors are obtained as [31, 47]

$$\vec{I}(x,y) = \frac{\mathrm{i}\omega}{2}\vec{u}(x,y)\cdot\mathbf{c}:\nabla\vec{u}^*(x,y)\,. \tag{4}$$

Let $\vec{I}_0(y) = \mathrm{Re}\,\vec{I}(0,y)$. The total time-averaged power flux through the plate in x-direction is obtained by integrating over the plate's cross section, i.e.,

$$P_{x0} = \int_{-h/2}^{h/2} \vec{I}_0(y)\cdot\vec{e}_x\,\mathrm{d}y\,. \tag{5}$$

For the differential section $\mathrm{d}x$ of the waveguide at $x = 0$, we can assume that

$$P_\mathrm{t} = P_{x0} + \left.\frac{\partial P_x(x)}{\partial x}\right|_{x=0}\mathrm{d}x = P_{x0} - 2\alpha P_{x0}\,\mathrm{d}x \tag{6}$$

and

$$\mathrm{d}P_\mathrm{r} = \vec{I}_0(h/2)\cdot\vec{e}_y\,\mathrm{d}x\,. \tag{7}$$

The balance of power flux $P_{x0} = P_\mathrm{t} + \mathrm{d}P_\mathrm{r}$ results in

$$\mathrm{d}P_\mathrm{r} = \vec{I}_0(h/2)\cdot\vec{e}_y\,\mathrm{d}x = -\left.\frac{\partial P_x(x)}{\partial x}\right|_{x=0}\mathrm{d}x\,, \tag{8}$$

i.e., the amount of power leaking into the fluid is equal to the decrease in power flux along the plate. Rearranging, we find that the radiation rate of leaky waves is

$$\alpha = \frac{\vec{I}_0(h/2)\cdot\vec{e}_y}{2P_{x0}}\,. \tag{9}$$

This calculation has been performed for all evanescent waves and the result is displayed together with the imaginary part of the wavenumbers in Fig. 10. Note the change in scale at 0.2 Np/mm for better visualization. The analysis leads to the following three findings:

5.2.1. Equivalence of attenuation and radiation rate

In Fig. 10, the radiation rate α coincides exactly with the imaginary part of the wavenumber spectrum, even for the evanescent waves with "high attenuation". It can be concluded that attenuation of quasi-guided waves in lossless media is *always* due to radiation.

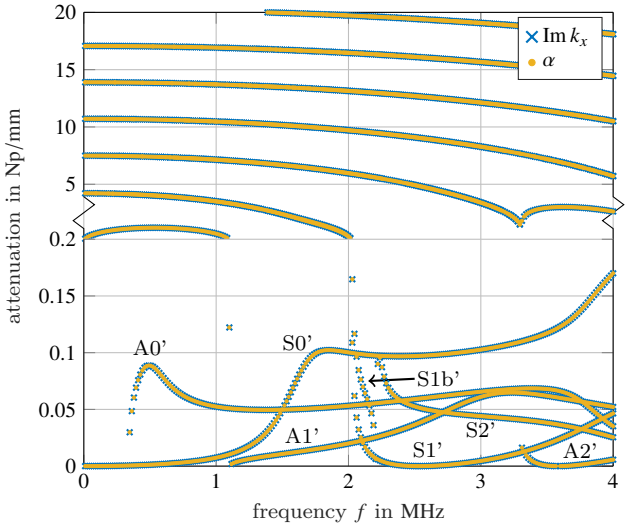

Figure 10: Comparison of the attenuation $\mathrm{Im}\, k_x$ and the radiation rate α as calculated by (9). For clarity, the plot has a change in scale at 0.2 Np/mm.

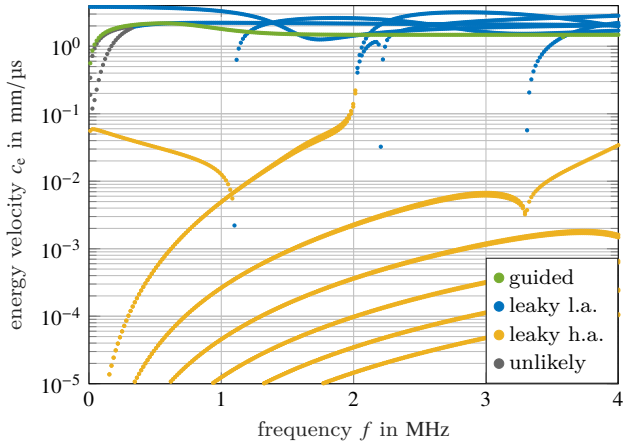

Figure 11: Energy velocity c_e of the water-coupled plate: modes with zero-energy velocity do not exist.

5.2.2. *Nonexistence of nonpropagating waves*

We observe that all waves have a well defined radiation rate α. According to (9), their power flux P_{x0} must be nonzero, which means that – in contrast to the free plate – nonpropagating modes do not exist. This result is analogous to the finding for lossy plates [24] and can be confirmed by inspecting the energy velocity c_e. We define the energy velocity as [14, 17, 19, 48]

$$c_e = \frac{P_{x0}}{\mathcal{H}_0}\,, \tag{10}$$

where $\mathcal{H}_0 = \mathcal{H}(x = 0)$ denotes the time-averaged total stored energy inside the plate at $x = 0$. It is obtained as the sum of kinetic energy $\mathcal{K}_0$ and elastic energy $\mathcal{E}_0$, i.e.,

$$\mathcal{H}_0 = \mathcal{K}_0 + \mathcal{E}_0\,, \tag{11}$$

with

$$\mathcal{K}_0 = \mathrm{Re} \int_{-h/2}^{h/2} \frac{\rho\omega^2}{4} \vec{u} \cdot \vec{u}^* \,\mathrm{d}y \tag{12}$$

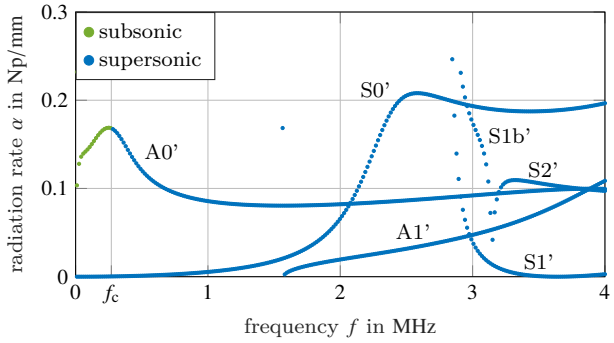

Figure 12: Radiation rate α of a 1 mm thick aluminum plate in contact on one side with water. Radiation extends well below the coincident frequency f_c.

and

$$\mathcal{E}_0 = \mathrm{Re} \int_{-h/2}^{h/2} \frac{1}{4} \nabla\vec{u} : \mathbf{c} : \nabla\vec{u}^* \,\mathrm{d}y\,. \tag{13}$$

The explicit computation of (13) is often avoided by exploiting the principle of equipartition of energy in lossless media [31], which states that $\mathcal{K}_0 = \mathcal{E}_0$. However, equipartition of energy does not hold for the open system under analysis [17]. Note also that in the above definition, only the plate is being considered part of the waveguide. It is still unclear if it is appropriate to neglect the fluid domain in the definition of energy velocity [17]. Nonetheless, it is deemed adequate to characterize the propagation of energy inside the plate [14, 17].

The energy velocity according to (10) has been computed for all eigensolutions and is plotted in logarithmic scale in Fig. 11. Contrary to the free plate, the energy velocity goes to zero only for singular points on the dispersion curves and, strictly speaking, zero-energy velocity modes do not exist. However, the present example is a "slightly fluid-loaded" plate and the energy velocity of the "quasi-nonpropagating" branches is very low, being consistent with the free plate model in the limit.

While the spectrum of the free plate splits clearly into propagating and nonpropagating modes, the eigensolutions of the fluid-coupled plate do not. Instead, the waves with high attenuation should be considered a continuation of the lowly attenuated ones – analogous to the finding by Simonetti and Lowe for free but lossy plates [24]. This is an important difference in the nature of the eigensolutions of the free and the fluid-coupled plate, as nonpropagating modes do not exist at all.

5.2.3. *Subsonic radiation*

It is often assumed a-priori that a guided wave with subsonic phase velocity, i.e., $c_p = \frac{\omega}{\mathrm{Re}\, k_x} < c_f$, where c_f is the fluid's wave speed, does not radiate an acoustic wave into the fluid [3, 7, 10, 14, 18, 20, 23, 45]. The above analysis rebuts this assumption. As an example, let us take a look at the radiation rate of an aluminum ($E = 70\,\mathrm{GPa}$, $\nu = 0.33$, $\rho = 2680\,\mathrm{kg/m^3}$) plate in contact on one side with water as depicted in Fig. 12. The coincident frequency, i.e., the frequency where the A0-mode of the free plate features the same phase velocity as the speed of sound in the fluid, has been marked in the figure. Below this frequency we find the subsonic region of the A0'-mode

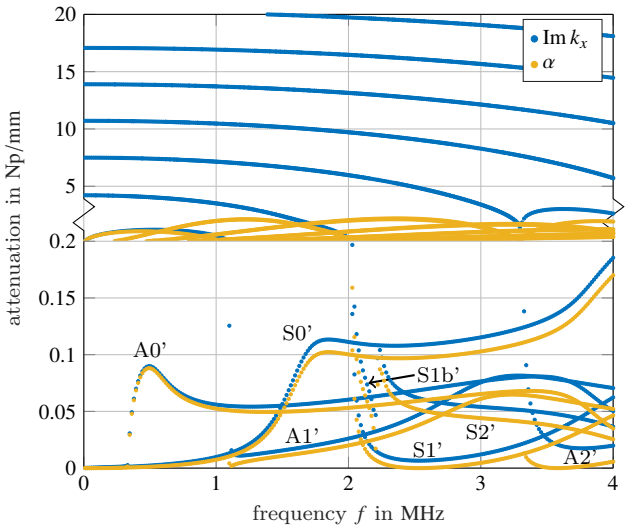

Figure 13: Viscoelastic 1 mm thick brass plate with single-sided water contact: comparison of the total attenuation Im k_x and the radiation rate α as calculated by (9). For clarity, the plot has a change in scale at 0.2 Np/mm.

and it can be observed that an acoustic wave is indeed radiated below coincidence. This is in agreement with previous findings [4, 49] and demonstrates that the concept of cut-off at the coincident frequency is merely an approximation and the result of a first-order perturbation of the free plate solution. For an accurate analysis of radiation it is necessary to actually solve the nonlinear leaky Lamb wave eigenvalue problem, as has been done in this contribution.

6. Viscoelastic plate coupled to water

As was shown above, for a perfectly elastic fluid-coupled plate, attenuation is solely due to radiation. This no longer holds for a lossy plate because damping of the plate's material leads to additional attenuation and an altered radiation rate. In order to demonstrate that this behavior can be considered with the presented modeling approach, we computed the leaky Lamb eigenvalue problem for a 1 mm thick brass plate with hysteretic damping [50, 51] (Young's modulus $E = 110(1 - \mathrm{i}0.0025)$GPa, Poisson's ratio $\nu = 0.34$, mass density $\rho = 8440\,\mathrm{kg/m^3}$). Fig. 13 displays the resulting attenuation Im k_x and the corresponding radiation rate α according to (9). As before, α is solely a consequence of leaked energy and, hence, characterizes the radiation process. Therefore, the radiation rate α allows to distinguish between the contributions of radiation and damping in the total attenuation Im k_x. Note that even for the lossy plate, it is sufficient to characterize leaky waves through Re $k_y > 0$, as it is equivalent to demanding a positive energy flux across the plate's boundaries, i.e., Re $\vec{I}_0(h/2) \cdot \vec{e}_y > 0$. It would not be possible, however, to separate leaky waves from incoming waves based solely on the wavenumbers k_x.

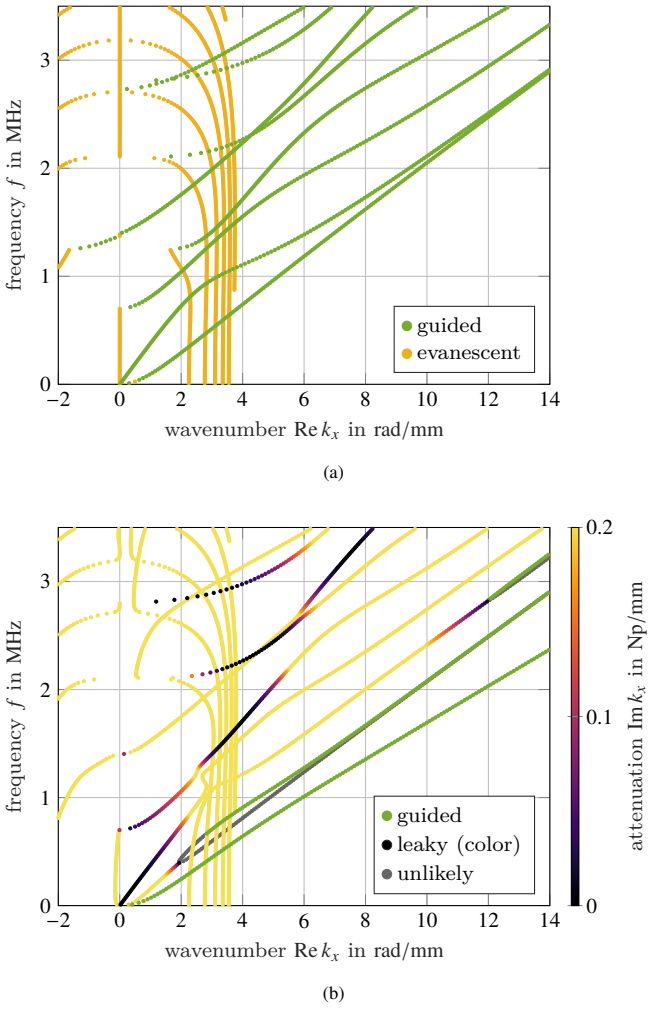

Figure 14: Comparison of the wavenumbers of a 1 mm thick PMMA plate: (a) traction free plate, (b) plate in contact with water on one side.

7. Strongly fluid-loaded plate

In general, the eigensolutions of the free and the fluid-coupled plate differ substantially. As our numerical solution procedure considers an exact plate-fluid interface condition, we are able to compute the exact eigensolutions of strongly fluid-loaded plates. Consider exemplarily a Poly(methyl methacrylate) (PMMA, acrylic glass) plate (Young's modulus $E = 6.17\,\mathrm{GPa}$, Poisson's ratio $\nu = 0.32$, mass density $\rho = 1190\,\mathrm{kg/m^3}$) coupled at one side to water. Note that in this case, the wave speed of transversal bulk waves c_t in the plate is lower than the fluid wave speed c_f. The resulting wavenumbers are displayed in Fig. 14b. Notice that the dispersion curves turn out to be quantitatively as well as qualitatively very different to the free plate's spectrum shown in Fig. 14a. For this reason, we no longer adopt the classification into "lowly attenuated" and "highly attenuated" waves. Above certain frequency, modes split into two real-valued branches that come close to each other for $f \to \infty$ and have, therefore, also been denoted as real-valued loops [44]. We remark that the lower branch lies on the negative imaginary line of the k_y-plane and we consider the solutions to be physically unlikely (Fig. 14b, ●). The same holds

for the first segment of the upper branch, while the following segment is a common guided wave solution (Fig. 14b, ●). This transition occurs where the phase velocity exhibits a maximum.

The above theoretical findings are in accordance with experimental results by Rostyne et al. [46]. However, for the best of the author's knowledge, the "higher-order Quasi-Scholte modes" have not been discussed in the literature previously. Note that in the far field of a source only the guided waves (●) and the leaky waves with low attenuation (dark color) are measurable inside the plate.

8. Conclusion

We discussed the dispersion curves and the wave field of plane harmonic waves in an elastic plate coupled to an inviscid fluid. The eigensolutions have been computed by solving the nonlinear leaky Lamb eigenvalue problem, which accounts for the analytically exact plate-fluid interaction. We find truly guided modes (trapped waves) that do not radiate into the fluid and are confined within the proximity of the plate. All other waves either radiate energy into the fluid (evanescent/leaky waves) or excite a wave inside the plate (incoming waves). We showed that the attenuation of waves in lossless media is always and solely due to radiation, that nonpropagating modes do not exist in the fluid-coupled plate, and that subsonic radiation is possible. The wave field's properties are strongly linked to the radiation rate and whether the wave is a forward or a backward wave.

Further studies could clarify the effect that damping inside the plate and/or the fluid domain has on the nature of quasi-guided waves. The nonpropagating modes of the free plate gain meaning through fluid-loading or damping. In a similar way, the physically unlikely solutions of a fluid-coupled plate could gain physical significance by adding appropriate material damping to the model.

Acknowledgments

The Chair of Sensor Technology is grateful for financial support by Diehl Metering.

References

[1] G. Lindner, Sensors and actuators based on surface acoustic waves propagating along solid–liquid interfaces, Journal of Physics D: Applied Physics 41 (12) (2008) 123002. doi:10.1088/0022-3727/41/12/123002.

[2] B. A. Auld, Acoustic Fields and Waves in Solids 2, 2nd Edition, Vol. 2, Krieger Publishing Company, Malabar, Fla, 1990.

[3] R. D. Watkins, W. H. B. Cooper, A. B. Gillespie, R. B. Pike, The attenuation of Lamb waves in the presence of a fluid, Ultrasonics 20 (6) (1982) 257–264. doi:10.1016/0041-624X(82)90046-4.

[4] H. Dabirikhah, C. W. Turner, The coupling of the A0 and interface Scholte modes in fluid-loaded plates, The Journal of the Acoustical Society of America 100 (5) (1996) 3442–3445. doi:10.1121/1.416985.

[5] M. O. Deighton, A. B. Gillespie, R. B. Pike, R. D. Watkins, Mode conversion of Rayleigh and Lamb waves to compression waves at a metal-liquid interface, Ultrasonics 19 (6) (1981) 249–258. doi:10.1016/0041-624X(81)90014-7.

[6] X. Jia, Modal analysis of Lamb wave generation in elastic plates by liquid wedge transducers, The Journal of the Acoustical Society of America 101 (2) (1997) 834–842. doi:10.1121/1.418041.

[7] S. I. Rokhlin, D. E. Chimenti, A. H. Nayfeh, On the topology of the complex wave spectrum in a fluid-coupled elastic layer, The Journal of the Acoustical Society of America 85 (3) (1989) 1074–1080. doi:10.1121/1.397490.

[8] V. Dayal, V. K. Kinra, Leaky Lamb waves in an anisotropic plate. I: An exact solution and experiments, The Journal of the Acoustical Society of America 85 (6) (1989) 2268–2276. doi:10.1121/1.397772.

[9] X. L. Bao, H. Franklin, P. K. Raju, H. Überall, The splitting of dispersion curves for plates fluid-loaded on both sides, The Journal of the Acoustical Society of America 102 (2) (1997) 1246–1248. doi:10.1121/1.419939.

[10] H. Dabirikhah, C. W. Turner, Anomalous behaviour of flexural waves in very thin immersed plates, in: IEEE 1992 Ultrasonics Symposium Proceedings, 1992, pp. 313–317 vol.1. doi:10.1109/ULTSYM.1992.275989.

[11] A. Freedman, Effects of fluid-loading on Lamb mode spectra, The Journal of the Acoustical Society of America 99 (6) (1996) 3488–3496. doi:10.1121/1.414948.

[12] D. A. Kiefer, M. Ponschab, S. J. Rupitsch, M. Mayle, Calculating the full leaky Lamb wave spectrum with exact fluid interaction, The Journal of the Acoustical Society of America 145 (6) (2019) 3341–3350. doi:10.1121/1.5109399.

[13] T. Hayashi, D. Inoue, Calculation of leaky Lamb waves with a semi-analytical finite element method, Ultrasonics 54 (6) (2014) 1460–1469. doi:10.1016/j.ultras.2014.04.021.

[14] M. Mazzotti, I. Bartoli, A. Marzani, E. Viola, A coupled SAFE-2.5D BEM approach for the dispersion analysis of damped leaky guided waves in embedded waveguides of arbitrary cross-section, Ultrasonics 53 (7) (2013) 1227–1241. doi:10.1016/j.ultras.2013.03.003.

[15] M. Gallezot, F. Treyssède, L. Laguerre, Contribution of leaky modes in the modal analysis of unbounded problems with perfectly matched layers, The Journal of the Acoustical Society of America 141 (1) (2017) EL16–EL21. doi:10.1121/1.4973313.

[16] F. Treyssède, K. L. Nguyen, A. S. Bonnet-BenDhia, C. Hazard, Finite element computation of trapped and leaky elastic waves in open stratified waveguides, Wave Motion 51 (7) (2014) 1093–1107. doi:10.1016/j.wavemoti.2014.05.003.

[17] I. A. Nedospasov, V. G. Mozhaev, I. E. Kuznetsova, Unusual energy properties of leaky backward Lamb waves in a submerged plate, Ultrasonics 77 (2017) 95–99. doi:10.1016/j.ultras.2017.01.025.

[18] E. V. Glushkov, N. V. Glushkova, O. A. Miakisheva, Backward waves and energy fluxes excited in acoustic medium with an immersed plate, Ultrasonics 94 (2019) 158–168. doi:10.1016/j.ultras.2018.10.001.

[19] A. Bernard, M. J. S. Lowe, M. Deschamps, Guided waves energy velocity in absorbing and non-absorbing plates, The Journal of the Acoustical Society of America 110 (1) (2001) 186–196. doi:10.1121/1.1375845.

[20] I. A. Viktorov, Rayleigh and Lamb Waves: Physical Theory and Applications, 2nd Edition, Ultrasonic technology, Plenum Press, New York, 1970.

[21] F. Hernando Quintanilla, M. J. S. Lowe, R. V. Craster, Full 3D dispersion curve solutions for guided waves in generally anisotropic media, Journal of Sound and Vibration 363 (2016) 545–559. doi:10.1016/j.jsv.2015.10.017.

[22] W. B. Fraser, Orthogonality relation for the Rayleigh–Lamb modes of vibration of a plate, The Journal of the Acoustical Society of America 59 (1) (1976) 215–216. doi:10.1121/1.380851.

[23] G. S. Kino, Acoustic Waves: Devices, Imaging, and Analog Signal Processing, Prentice Hall, Englewood Cliffs, N.J, 1987.

[24] F. Simonetti, M. J. S. Lowe, On the meaning of Lamb mode nonpropagating branches, The Journal of the Acoustical Society of America 118 (1) (2005) 186–192. doi:10.1121/1.1938528.

[25] C. Prada, D. Clorennec, D. Royer, Local vibration of an elastic plate and zero-group velocity Lamb modes, The Journal of the Acoustical Society of America 124 (1) (2008) 203–212. doi:10.1121/1.2918543.

[26] C. Grünsteidl, T. Berer, M. Hettich, I. Veres, Determination of thickness and bulk sound velocities of isotropic plates using zero-group-velocity Lamb waves, Applied Physics Letters 112 (25) (2018) 251905. doi:

10.1063/1.5034313.

[27] D. M. Stobbe, C. M. Grünsteidl, T. W. Murray, Propagation and Scattering of Lamb Waves at Conical Points in Plates, Scientific Reports 9 (1) (2019) 15216. doi:10.1038/s41598-019-51187-9.

[28] S. J. Rupitsch, Piezoelectric Sensors and Actuators - Fundamentals and Applications, 1st Edition, Topics in Mining, Metallurgy and Materials Engineering, Springer, Berlin Heidelberg, 2018.

[29] J. D. Achenbach, Wave Propagation in Elastic Solids, revised Edition, North Holland, Amsterdam, 1987.

[30] N. Marcuvitz, On field representations in terms of leaky modes or Eigenmodes, IRE Transactions on Antennas and Propagation 4 (3) (1956) 192–194. doi:10.1109/TAP.1956.1144410.

[31] K.-J. Langenberg, R. Marklein, K. Mayer, Theoretische Grundlagen der zerstörungsfreien Materialprüfung mit Ultraschall (Ultrasonic Nondestructive Testing of Materials: Theoretical Foundations), De Gruyter Oldenbourg, Munich, 2009.

[32] E. S. C. Ching, P. T. Leung, A. Maassen van den Brink, W. M. Suen, S. S. Tong, K. Young, Quasinormal-mode expansion for waves in open systems, Reviews of Modern Physics 70 (4) (1998) 1545–1554. doi:10.1103/RevModPhys.70.1545.

[33] P. T. Leung, S. Y. Liu, K. Young, Completeness and orthogonality of quasinormal modes in leaky optical cavities, Physical Review A 49 (4) (1994) 3057–3067. doi:10.1103/PhysRevA.49.3057.

[34] J. Hu, C. R. Menyuk, Understanding leaky modes: slab waveguide revisited, Advances in Optics and Photonics 1 (1) (2009) 58–106. doi:10.1364/AOP.1.000058.

[35] N. F. Declercq, R. Briers, J. Degrieck, O. Leroy, The history and properties of ultrasonic inhomogeneous waves, IEEE Transactions on Ultrasonics, Ferroelectrics, and Frequency Control 52 (5) (2005) 776–791. doi:10.1109/TUFFC.2005.1503963.

[36] K. L. Nguyen, F. Treyssède, C. Hazard, Numerical modeling of three-dimensional open elastic waveguides combining semi-analytical finite element and perfectly matched layer methods, Journal of Sound and Vibration 344 (2015) 158–178. doi:10.1016/j.jsv.2014.12.032.

[37] P. Zuo, Z. Fan, SAFE-PML approach for modal study of waveguides with arbitrary cross sections immersed in inviscid fluid, Journal of Sound and Vibration 406 (2017) 181–196. doi:10.1016/j.jsv.2017.06.001.

[38] P. T. Leung, W. M. Suen, C. P. Sun, K. Young, Waves in open systems via a biorthogonal basis, Physical Review E 57 (5) (1998) 6101–6104. doi:10.1103/PhysRevE.57.6101.

[39] M. Viens, Y. Tsukahara, C. K. Jen, J. D. N. Cheeke, Leaky torsional acoustic modes in infinite clad rods, The Journal of the Acoustical Society of America 95 (2) (1994) 701–707. doi:10.1121/1.408430.

[40] A. Grabówska, Propagation of elastic wave in solid layer-liquid system, Archives of Acoustics 4 (1) (1979) 57–63.

[41] H. Überall, B. Hosten, M. Deschamps, A. Gérard, Repulsion of phase-velocity dispersion curves and the nature of plate vibrations, The Journal of the Acoustical Society of America 96 (2) (1994) 908–917. doi:10.1121/1.411434.

[42] S. Tietze, G. Lindner, Visualization of the interaction of guided acoustic waves with water by light refractive vibrometry, Ultrasonics 99 (2019) 105955. doi:10.1016/j.ultras.2019.105955.

[43] J.-P. Sessarego, J. Sagéloli, C. Gazanhes, H. Überall, Two Scholte–Stoneley waves on doubly fluid-loaded plates and shells, The Journal of the Acoustical Society of America 101 (1) (1997) 135–142. doi:10.1121/1.418014.

[44] A. L. Shuvalov, O. Poncelet, M. Deschamps, Analysis of the dispersion spectrum of fluid-loaded anisotropic plates: flexural-type branches and real-valued loops, Journal of Sound and Vibration 290 (3) (2006) 1175–1201. doi:10.1016/j.jsv.2005.05.015.

[45] J. Dickey, G. Maidanik, H. Überall, The splitting of dispersion curves for the fluid-loaded plate, The Journal of the Acoustical Society of America 98 (4) (1995) 2365–2367. doi:10.1121/1.413283.

[46] K. V. d. Rostyne, C. Glorieux, a. W. Lauriks, J. Thoen, Experimental investigation of leaky Lamb modes by an optically induced grating, IEEE Transactions on Ultrasonics, Ferroelectrics, and Frequency Control 49 (9) (2002) 1245–1253. doi:10.1109/TUFFC.2002.1041541.

[47] B. A. Auld, Acoustic Fields and Waves in Solids 1, 2nd Edition, Vol. 1, Krieger Publishing Company, Malabar, Fla, 1990.

[48] K. J. Langenberg, R. Marklein, K. Mayer, Energy vs. group velocity for elastic waves in homogeneous anisotropic solid media, in: 2010 URSI International Symposium on Electromagnetic Theory, IEEE, Berlin, Germany, 2010, pp. 733–736. doi:10.1109/URSI-EMTS.2010.5637253.

[49] V. G. Mozhaev, M. Weihnacht, Subsonic leaky Rayleigh waves at liquid–solid interfaces, Ultrasonics 40 (1) (2002) 927–933. doi:10.1016/S0041-624X(02)00233-0.

[50] I. Bartoli, A. Marzani, F. Lanza di Scalea, E. Viola, Modeling wave propagation in damped waveguides of arbitrary cross-section, Journal of Sound and Vibration 295 (3) (2006) 685–707. doi:10.1016/j.jsv.2006.01.021.

[51] F. Hernando Quintanilla, Z. Fan, M. J. S. Lowe, R. V. Craster, Guided waves' dispersion curves in anisotropic viscoelastic single- and multi-layered media, Proc. R. Soc. A 471 (2183) (2015) 20150268. doi:10.1098/rspa.2015.0268.